

Magnesium–Antimony Liquid Metal Battery for Stationary Energy Storage

David J. Bradwell, Hojong Kim,* Aislinn H. C. Sirk,[†] and Donald R. Sadoway*

Department of Materials Science and Engineering, Massachusetts Institute of Technology, 77 Massachusetts Avenue, Cambridge, Massachusetts 02139-4307, United States

S Supporting Information

ABSTRACT: Batteries are an attractive option for grid-scale energy storage applications because of their small footprint and flexible siting. A high-temperature (700 °C) magnesium–antimony (Mg||Sb) liquid metal battery comprising a negative electrode of Mg, a molten salt electrolyte (MgCl₂–KCl–NaCl), and a positive electrode of Sb is proposed and characterized. Because of the immiscibility of the contiguous salt and metal phases, they stratify by density into three distinct layers. Cells were cycled at rates ranging from 50 to 200 mA/cm² and demonstrated up to 69% DC–DC energy efficiency. The self-segregating nature of the battery components and the use of low-cost materials results in a promising technology for stationary energy storage applications.

Large-scale energy storage is poised to play a critical role in enhancing the stability, security, and reliability of tomorrow's electrical power grid, including the support of intermittent renewable resources.¹ Batteries are appealing because of their small footprint and flexible siting; however, conventional battery technologies are unable to meet the demanding low-cost and long-lifespan requirements of this application.

A high-temperature (700 °C) magnesium–antimony (Mg||Sb) liquid metal battery comprising a negative electrode of Mg, a molten salt electrolyte (MgCl₂–KCl–NaCl), and a positive electrode of Sb is proposed (Figure 1). Because of density differences and immiscibility, the salt and metal phases stratify into three distinct layers. During discharge, at the negative electrode Mg is oxidized to Mg²⁺ (Mg → Mg²⁺ + 2e[−]), which dissolves into the electrolyte while the electrons are released into the external circuit. Simultaneously, at the positive electrode Mg²⁺ ions in the electrolyte are reduced to Mg (Mg²⁺ + 2e[−] → Mg_{Sb}), which is deposited into the Sb electrode to form a liquid metal alloy (Mg–Sb) with attendant electron consumption from the external circuit (Figure 2). The reverse reactions occur when the battery is charged. Charging and discharging of the battery are accompanied by volumetric changes in the liquid electrodes. The difference in the chemical potentials of pure Mg (μ_{Mg}) and Mg dissolved in Sb [$\mu_{\text{Mg(in Sb)}}$] generates a voltage that can be expressed as

$$E_{\text{cell}} = \frac{RT}{2F} \ln \left[\frac{a_{\text{Mg(in Sb)}}}{a_{\text{Mg}}} \right]$$

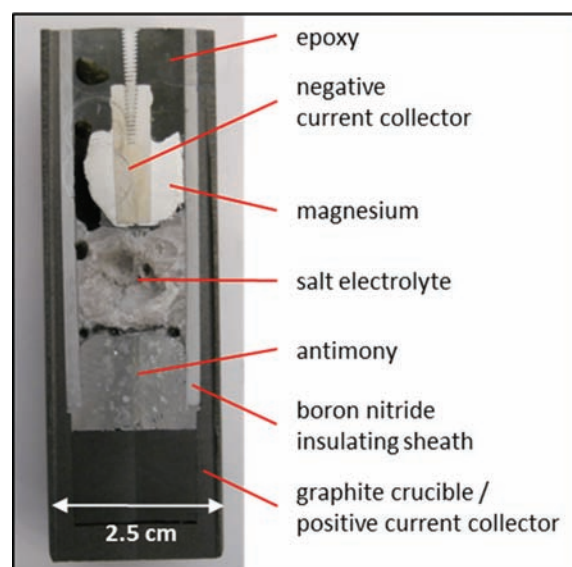


Figure 1. Sectioned Mg||Sb liquid metal battery operated at 700 °C showing the three stratified liquid phases upon cooling to room temperature. The cell was filled with epoxy prior to sectioning.

where R is the gas constant, T is temperature in Kelvins, F is the Faraday constant, $a_{\text{Mg(in Sb)}}$ is the activity of Mg dissolved in Sb, and a_{Mg} is the activity of pure Mg.

Recent work on self-healing Li–Ga electrodes for lithium ion batteries has demonstrated the appeal of liquid components.² While solid electrodes are susceptible to mechanical failure by mechanisms such as electrode particle cracking,³ these are inoperative in liquid electrodes, potentially endowing cells with unprecedented lifespans. The self-segregating nature of liquid electrodes and electrolytes could also facilitate inexpensive manufacturing of a battery so constructed. However, there do not appear to be economical materials options that exist as liquids at or near room temperature.

Previous work with elevated-temperature liquid batteries demonstrated impressive current density capabilities (>1000 mA/cm² when discharged at 0 V) with a variety of chemistries.^{4–7} However, that work generally used prohibitively expensive metalloids (such as Bi and Te) as the positive electrode. The resulting cells exhibited self-discharge current densities of 40 mA/cm², attributed to the solubility of the negative electrode metal (i.e., Na) in the

Received: October 17, 2011

Published: January 6, 2012

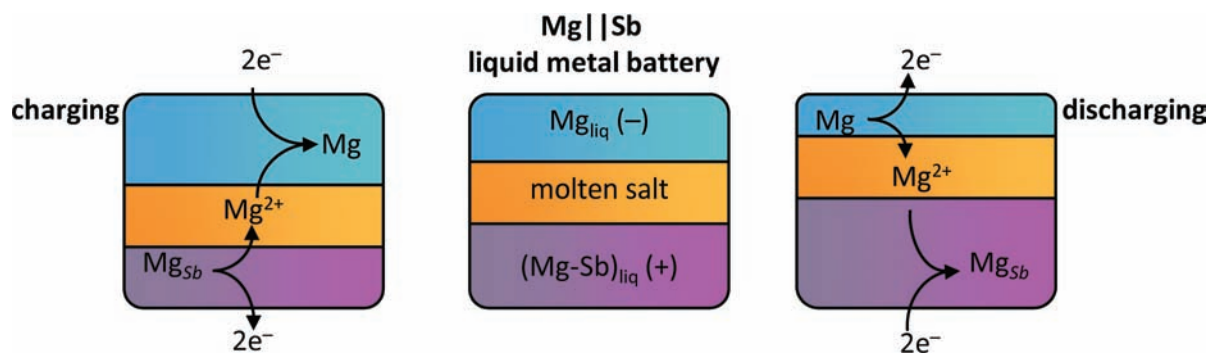


Figure 2. Schematic of a Mg||Sb liquid metal battery comprising three liquid layers that operates at 700 °C. During charging, Mg is electrochemically extracted from the Mg–Sb alloy electrode and deposited as liquid Mg on the top (negative) electrode. During discharging, the Mg electrode is consumed, and Mg is deposited into the Mg–Sb liquid bottom (positive) electrode. During charging, the battery consumes energy; upon discharge, the battery supplies energy.

electrolyte.⁵ These systems failed to achieve commercial success, possibly because of a lack of interest in grid-scale storage at that time or the use of high-cost metalloids.

Sb is less costly (\$7/kg average commodity price over the past 5 years) and more earth-abundant than Bi (\$24/kg) and Te (\$150/kg).⁸ When costs are compared on a per-mole basis (which is more relevant when considering the cost per unit of energy storage capacity), Sb (\$0.74/mol) appears even more appealing than Bi (\$4.40/mol) and Te (\$19.19/mol). Interestingly, the use of Sb had not, until now, been demonstrated in a liquid metal battery.

Mg was selected as the negative electrode material on the basis of its low cost (\$5.15/kg, \$0.125/mol), high earth abundance, low electronegativity, and overlapping liquid range with both Sb and candidate electrolytes. The electrolyte was MgCl₂:NaCl:KCl (50:30:20 mol %), which was selected on the basis of its sufficiently low melting point (396 °C⁹) and the greater electrochemical stability of NaCl and KCl in comparison with MgCl₂.¹⁰

Mg||Sb single cell batteries were assembled in the fully charged state in an Ar-filled glovebox, placed inside a sealed test vessel, and heated in a vertical tube furnace to 700 °C. When the cell was heated above the melting point of the molten salt, cell open-circuit voltages were found to stabilize at ~0.44 V, consistent with thermodynamic data.¹¹

The cells were electrochemically characterized by cyclic voltammetry (CV) and electrochemical impedance spectroscopy (EIS) using a two-electrode electrochemical setup with the negative electrode (Mg) as the counter electrode/reference electrode and the positive electrode (Sb) as the working electrode. The cells exhibited negligible charge-transfer overpotentials, as demonstrated by the linearity of the current–voltage relationship in the CV scans and the absence of an obvious semicircle in the EIS scans. The slope of the CV was consistent with the area-normalized solution resistance as measured through EIS (typically 1.1 Ω cm²), further demonstrating IR voltage loss to be the dominant overpotential.

There were, however, indications of mass-transport limitations under certain conditions. The cells exhibited increased cell impedance at lower EIS scan frequencies, suggesting that at long time periods the reaction rates might be limited by diffusion.¹² Mass-transport limitations could arise from local depletion of Mg²⁺ ions in the electrolyte at either of the electrode–electrolyte interfaces or Mg mass-transport limitations in the Mg–Sb electrode at the Mg–Sb electrode/electrolyte interface.

Further electrochemical characterization was performed. Stepped-potential experiments indicated low leakage current densities of <1 mA/cm², well below those of previously studied systems. This was attributed to the complexation of Mg²⁺ by ligand donors from the supporting electrolyte (NaCl, KCl)¹³ and the attendant suppression of metal solubility in its halide salts.¹⁴

Cells cycled at 50 mA/cm² for a predefined discharge period of 10 h to a cutoff charging voltage limit of 0.85 V achieved a round-trip Coulombic efficiency of 97% and a voltage efficiency of 71%, resulting in an overall energy efficiency of 69% (Figure 3a).

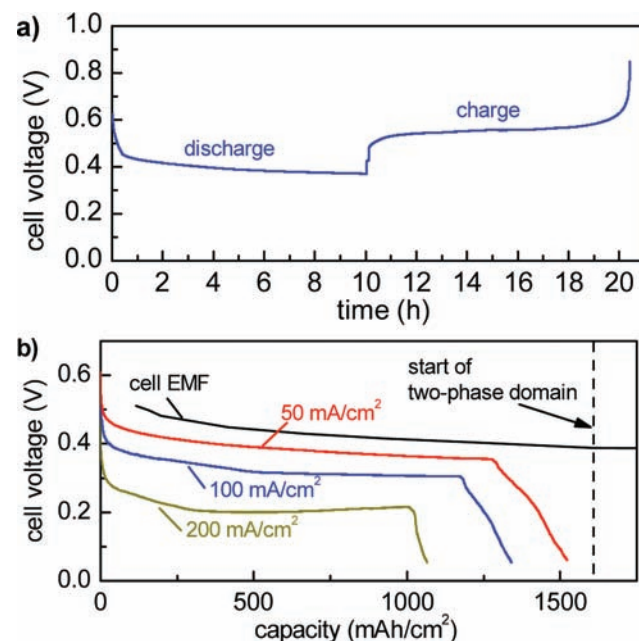


Figure 3. Electrochemical performance of a Mg||Sb liquid metal battery operated at 700 °C. (a) Variation of the cell voltage with the state of charge over one cycle. The current was set at 50 mA/cm². (b) Deep discharge results at different current rates. The theoretical cell EMF was calculated from data in the literature.¹¹

At full discharge, the composition of the positive (bottom) liquid electrode was estimated to be 12 mol % Mg and 88 mol % Sb.

Cells were fully discharged at various rates ranging from 50 to 200 mA/cm² with 0.05 V as the discharge cutoff limit (Figure 3b). Operation at higher current density resulted in increased IR voltage loss and decreased capacity, consistent

with the measured solution resistance and observed mass-transport limitations. The operating efficiency could be improved by reducing the thickness of the electrolyte or operating at lower current density. The cell performance could be optimized by changes in the current collector design and in the electrolyte composition to increase the cell conductivity.

Cells were cycled more than 30 times for periods of up to 2 weeks and did not exhibit obvious signs of corrosion of the solid-state cell components (current collectors and walls), as determined through optical imaging and scanning electron microscopy (SEM)/energy-dispersive spectroscopy (EDS) analysis. Analysis of the positive electrodes of cells that were cooled in a discharged state revealed the presence of Mg platelets, consistent with the formation of Mg_3Sb_2 (Figure 4).

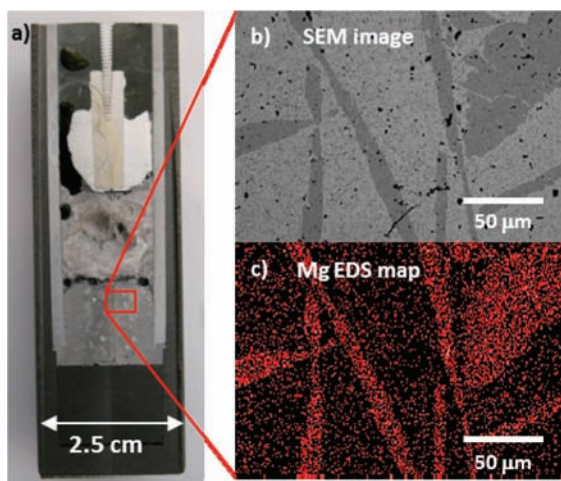


Figure 4. (a) Cross section of a Mg||Sb cell. (b) SEM image of a positive electrode in the discharged state. (c) Mg EDS map showing high Mg concentrations in sectioned platelets.

The Mg–Sb phase diagram indicates that a two-phase microstructure is to be expected as a result of phase separation as the electrode is cooled from a Mg–Sb single-phase liquid regime into a two-phase Sb and Mg_3Sb_2 regime.

Stationary storage applications require devices to operate reliably for many years. In the present study, corrosion was not an issue. However, after several weeks of cycling, the cells ceased to operate. The observed cause of failure was evaporation of the molten salt electrolyte into the surrounding containment vessel, a mechanism that could be mitigated by alternative cell designs with reduced head space.

In summary, an all-liquid battery with Mg and Sb liquid metal electrodes has been proposed and its performance capability demonstrated. The use of Sb as the positive electrode and the self-segregating nature of the liquid components may enable a low-cost energy storage solution. Cells were cycled under constant-current conditions, demonstrating high current density capabilities and negligible corrosion of the solid-state cell components over the testing period.

Further work is required for evaluation of the long-term performance of the proposed cells, which may require an alternative cell design. At some larger scale, the action of electric current flowing through the electrolyte could generate enough Joule heat to keep the components molten, thereby obviating the need for external heaters, as is the case with electrolytic cells producing aluminum on a commercial scale.¹⁵

Future work will include long-term corrosion testing of solid-state components, current collector optimization, and investigation of alternative sheath materials. While the initial cell performance results are promising, exploration of other metal–metalloid couples with still greater cell voltages and lower operating temperatures is warranted. If a low-cost, high-voltage system with sufficiently low levels of corrosion were discovered, it would find utility in a wide array of stationary storage applications.

■ ASSOCIATED CONTENT

📄 Supporting Information

Experimental procedures, cell design details, heating profile, materials selection, and additional electrochemical results. This material is available free of charge via the Internet at <http://pubs.acs.org>.

■ AUTHOR INFORMATION

Corresponding Author

hojong@mit.edu; dsadoway@mit.edu

Present Address

[†]Department of Law, University of Victoria, Victoria, BC, Canada.

■ ACKNOWLEDGMENTS

Financial support from the Deshpande Center for Technological Innovation at MIT, the Chesonis Family Foundation at MIT, the Advanced Research Projects Agency-Energy (U.S. Department of Energy), and Total, S.A. is gratefully acknowledged.

■ REFERENCES

- (1) *Advanced Electricity Storage Technologies Programme. Energy Storage Technologies: A Review Paper*; Australian Greenhouse Office, Department of the Environment and Heritage: Commonwealth of Australia, 2005.
- (2) Deshpande, R. D.; Li, J.; Cheng, Y. T.; Verbrugge, M. W. *J. Electrochem. Soc.* **2011**, *158*, A845.
- (3) Christensen, J.; Newman, J. J. *Solid State Electrochem.* **2006**, *10*, 293.
- (4) Shimotake, H.; Rogers, G. L.; Cairns, E. J. *Ind. Eng. Chem. Process Des. Dev.* **1969**, *8*, 51.
- (5) Cairns, E. J.; Shimotake, H. *Prepr. Pap.—Am. Chem. Soc., Div. Fuel Chem.* **1967**, *11* (3), 321.
- (6) Shimotake, H.; Cairns, E. J. In *Proceedings of the Intersociety Energy Conversion Engineering Conference*; American Society of Mechanical Engineers: New York, 1967.
- (7) Cairns, E. J.; Shimotake, H. *Science* **1969**, *164*, 1347.
- (8) *Mineral Commodity Summaries 2011*; U.S. Geological Survey: Reston, VA, 2011.
- (9) Janecke, E. Z. *Anorg. Allg. Chem.* **1950**, *261*, 218.
- (10) Plambeck, J. A.; Bard, A. J. *Encyclopedia of Electrochemistry of the Elements*; Marcel Dekker: New York, 1976; Vol. X, pp 127–148.
- (11) Eckert, C.; Irwin, R.; Smith, J. *Metall. Mater. Trans. B* **1983**, *14*, 451.
- (12) Bard, A.; Faulkner, L. *Electrochemical Methods: Fundamentals and Applications*, 2nd ed.; Wiley: New York, 2001.
- (13) Brooker, M.; Huang, C. *Can. J. Chem.* **1980**, *58*, 168.
- (14) Mulcahy, M. F. R.; Heymann, E. J. *Phys. Chem.* **1943**, *47*, 485.
- (15) Haupin, W.; Frank, W. *Comprehensive Treatise of Electrochemistry*; Plenum Press: New York, 1981; Vol. 2, pp 301–325.